

DESY 04–105
June 2004

Bremsstrahlung in Leptonic Onia Decays: Effects on Mass Spectra

*Alexander Spiridonov**

DESY Zeuthen

Abstract

In this note we present a study of the radiative tails in the invariant mass spectra of muon or electron pairs from J/ψ , $\psi(2S)$ and $\Upsilon(1S)$ decays which is due to an additional emission of a photon. An analytic formula for dilepton mass spectra in radiative decays is derived and a Monte Carlo simulation for realistic detector conditions is used to study effects on the spectra. A rather simple parameterisation is given, suitable for the treatment of real data.

*Permanent address: Institute of Theoretical and Experimental Physics, 117259 Moscow, Russia

1 Introduction

The prediction from the Standard Model for radiative decays of Z bosons into lepton pairs was discussed by Fleischer and Jegerlehner [1] and analytic results for the photon emission valid for arbitrary cuts on photon energies and angles have been presented. The lowest order decay width $\Gamma_0(Z \rightarrow l^+l^-)$ and contributions from radiative corrections were factorised in the presented formulae. We used the same formulae with appropriate mass parameters to estimate the radiative effects for heavy vector mesons decaying into lepton pairs.

Radiative effects in the context of the bottomonia spectroscopy were discussed in details by Buchmüller and Cooper [2] with a clear recommendation (p.427) that the experimental definition of $\Upsilon \rightarrow e^+e^-$ should include all $\Upsilon \rightarrow e^+e^-\gamma$ decays in order to avoid sensitivity to a cut in the photon energy. Certainly that should be valid also for charmonia decays and for $\mu^+\mu^-$ and $\mu^+\mu^-\gamma$ final states, respectively. There are no principal differences between these cases, besides the level of the radiative effects.

The first observation [3] of the radiative decay $J/\psi \rightarrow e^+e^-\gamma$, where the branching ratio $B(J/\psi \rightarrow e^+e^-\gamma, E_\gamma > 100 \text{ MeV})$ divided by the branching ratio $B(J/\psi \rightarrow e^+e^-)$ was measured as 0.147 ± 0.022 , is in good agreement with the expectation. The theoretical prediction based on results [1] for the corresponding decay into muons is smaller by a factor about 3 only, i.e. also rather large. Radiative tails could be statistically significant in inclusive mass spectra of lepton pairs from decays of J/ψ in measurements with high statistics and rather good mass resolution like in the HERA-B experiment [4].

We derive an analytic formula for the dilepton invariant mass spectra in radiative decays. In practice, a convolution of such ideal spectrum with detector mass resolution should be taken into account. We investigated the smearing effects by Monte Carlo simulation taking into account realistic detector conditions for the J/ψ , $\psi(2S)$ and $\Upsilon(1S)$ decays into $\mu^+\mu^-\gamma$ or $e^+e^-\gamma$. A simple parameterisation was found to describe simulated dilepton mass spectra for different mass resolutions. The parameterisation fitted rather well the simulated mass spectra and was appropriate for fitting of real dimuon spectra from J/ψ decays.

2 Photon Emission in Decays into Lepton Pairs

In [1] radiative decays of Z bosons were considered and analytic results for arbitrary cuts on the photon energy and on the angles between photon and leptons were presented. The authors included the complete one-loop electroweak corrections and multi-soft-photon effects. The photons (real or virtual) could be emitted and absorbed only by the final state leptons. The effect of the initial state entered only via the phase space boundaries given by its mass, therefore only the mass of the decaying particle entered into the expressions for radiative corrections and the lowest order decay width $\Gamma_0(Z \rightarrow l^+l^-)$ was used as a normalisation factor. We used the appropriate formulas from [1] to study radiative decays of heavy vector mesons into lepton pairs.

Let us consider the decay $X \rightarrow l^+l^-$ of a heavy vector state with mass M into a pair of leptons with masses m_l . The lowest order decay width is

$$\Gamma_0 = \Gamma_0(X \rightarrow l^+l^-). \quad (1)$$

The bremsstrahlung process

$$X(p_0) \rightarrow l^-(p_1) + l^+(p_2) + \gamma(k) \quad (2)$$

is distributed in the phase space as [1]:

$$\begin{aligned} \frac{1}{\Gamma_0} \frac{d^2\Gamma(X \rightarrow l^+l^-\gamma)}{d\varsigma d\tau} &= P(\varsigma, \tau) \\ &= \frac{\alpha}{2\pi} \left[\left(\frac{1+\varsigma^2}{1-\varsigma} \right) \left(\frac{1}{\tau} + \frac{1}{1-\varsigma-\tau} \right) - \frac{a}{2} \left(\frac{1}{\tau^2} + \frac{1}{(1-\varsigma-\tau)^2} \right) - 2 \right], \end{aligned} \quad (3)$$

where α is the fine structure constant, $\varsigma = (p_1 + p_2)^2/M^2$, $\tau = (p_0 - p_1)^2/M^2$ and $a = 4m_l^2/M^2$, $a \leq \varsigma \leq 1$.

In the rest frame of the decaying particle we have $\varsigma = 1 - 2E_\gamma/M$, $\tau = 1 - 2E_1/M$ and $1 - \varsigma - \tau = 1 - 2E_2/M$, and in the center of mass system of the lepton pair:

$$\tau = 1 - \varsigma - \frac{1}{2}(1 - \varsigma)(1 - r \cos \theta_1) \quad \text{or} \quad \tau = \frac{1}{2}(1 - \varsigma)(1 - r \cos \theta_2)$$

with $r = \sqrt{1 - a/\varsigma}$ and θ_i the angle between the photon and lepton with momentum \vec{p}_i , obviously $\theta_1 = \pi - \theta_2$. Variations of θ_2 from $\theta_2 = 0$ to $\theta_2 = \pi$ corresponds to

$$\tau(0) = \frac{1}{2}(1 - \varsigma)(1 - r), \quad \tau(\pi) = \frac{1}{2}(1 - \varsigma)(1 + r).$$

The parameter ς is related to the invariant mass of the lepton pair:

$$m^2 = (p_1 + p_2)^2 = \varsigma \cdot M^2.$$

The distribution $P(\varsigma)$ can be evaluated by integrating the distribution $P(\varsigma, \tau)$ over the parameter τ :

$$\begin{aligned} \frac{1}{\Gamma_0} \frac{d\Gamma(X \rightarrow l^+l^-\gamma)}{d\varsigma} &= P(\varsigma) = \int_{\tau(0)}^{\tau(\pi)} P(\varsigma, \tau) d\tau \\ &= \frac{\alpha}{\pi} \frac{1+\varsigma^2}{1-\varsigma} \left(\ln \frac{1+r}{1-r} - r \right), \end{aligned} \quad (4)$$

The latter formula agrees with the expression $P(\varsigma, > \delta)$ from [1] in the limit $\delta = 0$ presenting the result of integration of $P(\varsigma, \tau)$ over the angles θ_1, θ_2 with exclusion of cones around the leptons defined by the angle δ .

Photons with sufficient energy can be detected. The fraction of decays corresponding to the emission of hard photons is

$$C_{hard}(E_{min}) = \frac{1}{\Gamma_0} \cdot \Gamma(X \rightarrow l^+l^-\gamma, E_\gamma > E_{min}) = \int_a^{1-2E_{min}/M} P(\varsigma) d\varsigma, \quad (5)$$

where E_{min} is the minimal photon energy in the rest frame of the decaying particle. The result of integration for $E_{min} \ll M/2$, neglecting terms of order $O(\alpha\alpha)$, is known [1]:

$$C_{hard}(E_{min}) = \frac{\alpha}{2\pi} \left[4 \ln \frac{M}{2E_{min}} \left(\ln \frac{M^2}{m_l^2} - 1 \right) - 3 \ln \frac{M^2}{m_l^2} - \frac{2}{3}\pi^2 + \frac{11}{2} \right]. \quad (6)$$

The measurement of $J/\psi \rightarrow e^+e^-\gamma$ [3] is in good agreement with the calculation C_{hard} in fig. 1.

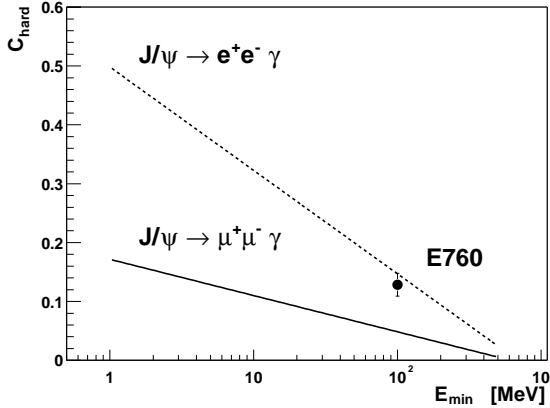


Figure 1: Parameter C_{hard} as a function of the minimal energy E_{min} of the photon in the J/ψ rest frame for radiative decays $J/\psi \rightarrow \mu^+\mu^-\gamma$ (solid line) and $J/\psi \rightarrow e^+e^-\gamma$ (dashed line). The point with errors was evaluated from the E760 result [3].

The lepton mass entered in eq. 6 in the first (leading) term as $\ln(M^2/m_l^2)$ which is smaller only by a factor 2.6 for muons compared to electrons. The effect of hard photon emission is expected to be rather large also for decays into $\mu^+\mu^-\gamma$ as shown in fig. 1. The effects are larger for heavier decaying particles as seen in fig. 2 comparing J/ψ , $\psi(2S)$ and $\Upsilon(1S)$, respectively.

In order to get the physical rate, we have to take into account contributions from virtual photons (emitted and absorbed by leptons) and emitted soft photons ($E_\gamma < E_{min}$). The sum of these contributions is known [1]:

$$C_{soft}(E_{min}) = \frac{\alpha}{2\pi} \left[-4 \ln \frac{M}{2E_{min}} \left(\ln \frac{M^2}{m_l^2} - 1 \right) + 3 \ln \frac{M^2}{m_l^2} + \frac{2}{3}\pi^2 - 4 \right]. \quad (7)$$

The total width taking into account l^+l^- , $l^+l^-\gamma$ configurations is

$$\Gamma_{all}(X \rightarrow l^+l^-, l^+l^-\gamma) = (1 + C_{soft} + C_{hard}) \cdot \Gamma_0(X \rightarrow l^+l^-). \quad (8)$$

The term C_{soft} is negative as seen in fig. 3. The leading terms in C_{soft} and C_{hard} have singular behavior for $E_{min} \rightarrow 0$, but in the sum $C_{soft} + C_{hard}$ they exactly cancel, as it should be:

$$C_{soft} + C_{hard} = \frac{\alpha}{2\pi} \frac{3}{2}. \quad (9)$$

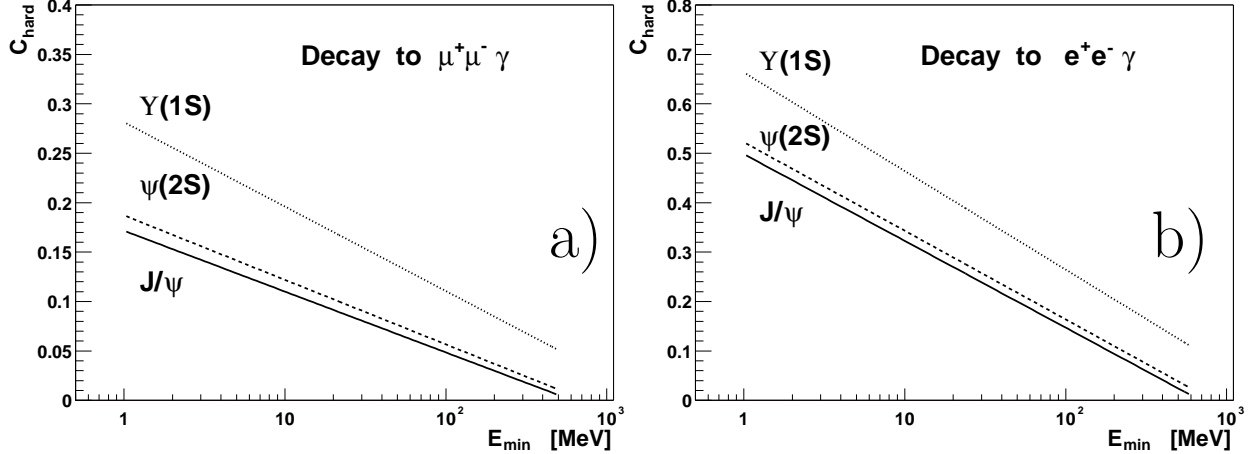


Figure 2: The parameter C_{hard} as a function of the minimal energy E_{min} of the photon in the rest frame of J/ψ (solid line), $\psi(2S)$ (dashed line), and $\Upsilon(1S)$ (dotted line) decaying into $\mu^+\mu^-\gamma$ (a) or $e^+e^-\gamma$ (b).

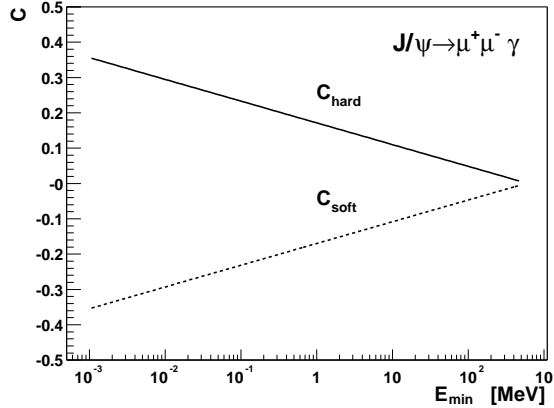


Figure 3: The parameters C_{hard} (solid line) and C_{soft} (dashed line) for the radiative decay $J/\psi \rightarrow \mu^+\mu^-\gamma$ as functions of the minimal photon energy E_{min} in the rest frame of the J/ψ .

When an experiment measures all l^+l^- , $l^+l^-\gamma$ configurations independent of the energy of emitted photons, the effects of radiative corrections appear as a small increase of the decay width

$$\frac{\Gamma_{all} - \Gamma_0}{\Gamma_0} = \frac{\alpha}{2\pi} \frac{3}{2} \approx 0.00174. \quad (10)$$

However, cuts on the energy of the emitted photon can have much stronger effect. Let us assume that we are selecting lepton pairs inclusively and apply a cut on their invariant mass

$$|m - M| < \Delta.$$

The radiative decays with photon energies in the rest frame of the decay

$$E_\gamma > E_\Delta = \Delta \left(1 - \frac{\Delta}{2M}\right) \quad (11)$$

will be rejected and the number of selected decays will be reduced by the factor

$$\frac{N(l^+l^-, |m - M| < \Delta)}{N(l^+l^-)} = \frac{(1 + C_{soft}(E_\Delta))}{\left(1 + \frac{\alpha}{2\pi} \frac{3}{2}\right)}. \quad (12)$$

For inclusive registration of $\mu^+\mu^-$ pairs from J/ψ decays and the rather soft cut $\Delta = 200$ MeV, about 3% of the decays will be rejected. In general, the dilepton mass m is shifted by photon emission

$$m = \sqrt{M(M - 2E_\gamma)} \approx M - E_\gamma \quad (E_\gamma \ll M). \quad (13)$$

Hard photon emission causes a tail towards lower masses in the dilepton mass spectrum.

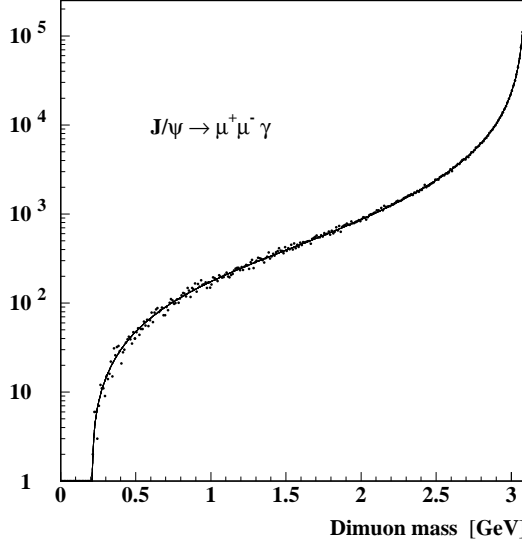


Figure 4: The dimuon mass spectrum defined by eq. 14 (solid line) and results of Monte Carlo simulation (points) of the decay $J/\psi \rightarrow \mu^+\mu^-\gamma$ for an ideal detector (without smearing, 4π acceptance) for $E_{min} = 10$ MeV.

The distribution $P(m)$ of the dilepton mass in the radiative decay (2) we find from eq. (4) as

$$\frac{1}{\Gamma_0} \frac{d\Gamma(X \rightarrow l^+l^-\gamma)}{dm} = P(m) = \frac{\alpha}{\pi} \frac{2m}{(M^2 - m^2)} \left(1 + \frac{m^4}{M^4}\right) \left(\ln \frac{1+r}{1-r} - r\right), \quad (14)$$

where $r = \sqrt{1 - 4m_l^2/m^2}$ is also a function of m . The singular behavior of the spectrum for $E_\gamma \rightarrow 0$ ($m \rightarrow M$) is clearly seen in fig. 4.

In an experiment which measures the dilepton mass spectrum inclusively a separation of l^+l^- and $l^+l^-\gamma$ final states is not possible on an event by event basis. For very low photon energies that is not possible even on a statistical basis, because both decays contribute to the peak around the mass of the decaying particle. The measured spectrum can be described by two components. The main component corresponds to decays into l^+l^- and $l^+l^-\gamma$ ($E_\gamma \leq E_{min}$) contributing to a “monochromatic” line ($m = M$) in dilepton mass spectrum smeared by detector resolutions. An additional component is related to the $l^+l^-\gamma$ ($E_\gamma > E_{min}$) final states producing the spectrum (14) also affected by detector resolutions. The fraction of events in the latter component is

$$W_{hard} = \frac{C_{hard}(E_{min})}{1 + \frac{\alpha}{2\pi} \frac{3}{2}}. \quad (15)$$

3 Smearing Effects due to Detector Resolutions

After smearing due to limited detector resolutions, the shape of the dilepton mass spectrum from radiative decay (14) changes in particular for low energy photons ($m \approx M$) as seen in fig. 5. The spectrum (14) convoluted with the Gaussian could not be expressed in an analytic form and in addition, experimental cuts complicate the situation even more.

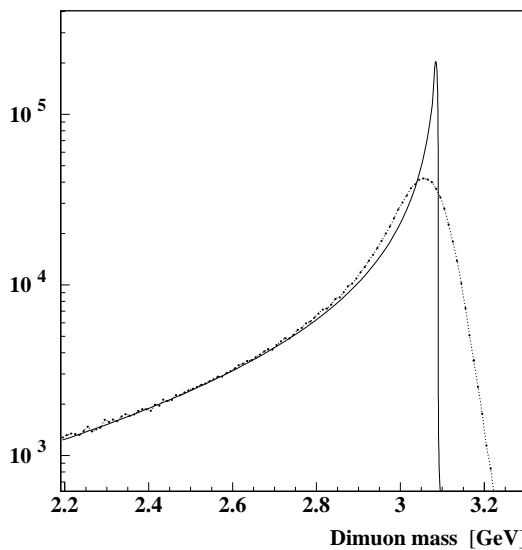


Figure 5: Dimuon mass spectra in the radiative decay $J/\psi \rightarrow \mu^+\mu^-\gamma$ for $E_{min} = 10$ MeV (solid line) smeared with mass resolution of about 42 MeV (points connected by dashed line).

Our goal was to derive a function to be used in fitting the spectra. We investigated radiative decays by Monte Carlo simulation for real experimental conditions and propose a rather simple parameterisation for smeared dilepton mass spectra. We used the Monte

Carlo generator for simulation of the kinematics of the decay (2) developed by Lohse [5] and based on the results in [1]. The generated spectrum of the dilepton invariant mass was in good agreement with the analytic expression (14) as shown in fig. 4. To study the real experimental conditions we simulated radiative decay within the framework of the HERA-B detector. Protons with an energy of 920 GeV colliding with a nuclear target directly produced the J/ψ (or $\psi(2S)$, $\Upsilon(1S)$). The distributions of the transverse momentum p_T and the Feynman scaling variable x_F were generated according to the model described in [6]. The particle decayed into $\mu^+\mu^-(e^+e^-)$ or $\mu^+\mu^-\gamma(e^+e^-\gamma)$ with a probability determined by the cut parameter E_{min} , the minimal energy of the photon in the rest frame of the decay.

The HERA-B detector is a forward spectrometer with a tracking system including the vertex detector placed in front of the magnet and main tracker system behind the magnet. The electro-magnetic calorimeter and muon system located behind the main tracker are used for particle identification and triggering. The main tracker includes the inner and outer trackers, but only the latter was taken into account since only this part was used in the dilepton trigger. Events where the both leptons passed through the tracking and particle identification detectors were considered. The trigger also imposed cuts on leptons, e.g. only muons with energy higher than 6 GeV were selected.

The momentum resolution for muons was simulated according to the parameterisation [7]

$$\frac{\sigma(p)}{p}(\%) = 0.94 \oplus 9.55 \cdot 10^{-3} \cdot p \oplus 0.484 \cdot p^{0.263}, \quad (16)$$

where p is in GeV. We were interested to isolate effects induced by the internal bremsstrahlung in decays and therefore did not simulate bremsstrahlung photons from electrons on the path through the detector material. The simulated momentum resolution for electrons was the same as for muons. To study dilepton spectra for various resolutions we multiplied eq. 16 by fudge factors from 0.7 up to 2.5. That corresponded to the variation of mass resolution at the J/ψ peak from 23 MeV up to 81 MeV, respectively.

The decays corresponding to $E_\gamma \leq E_{min}$ were simulated as l^+l^- final states smeared by detector resolutions. The remaining part of the spectrum consisted of simulated $l^+l^-\gamma$ configurations ($E_\gamma > E_{min}$), also affected by detector resolutions. Our aim was to find a simple analytic approximation for the latter part of the simulated spectrum with the additional condition that the mass resolution can also be treated as unknown and included in the fit parameters. We solved this problem in three steps:

- Find the value E_{min} appropriate for the simulation;
- Define a parameterisation for the smeared dilepton mass spectra in the radiative decays;
- Determine the corresponding parameters as functions of the mass resolution.

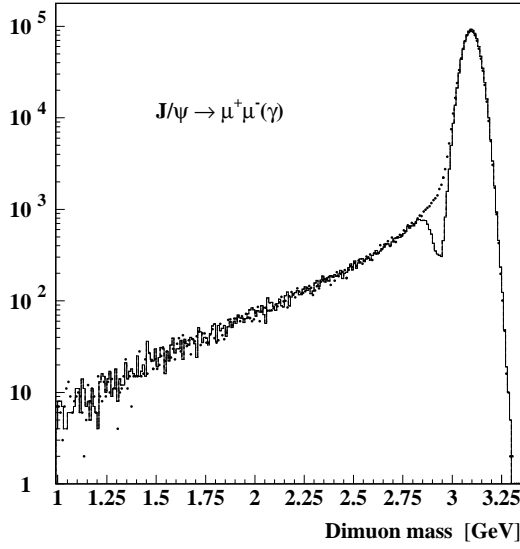


Figure 6: Dimuon mass spectra simulated by Monte Carlo for the mixture of $J/\psi \rightarrow \mu^+\mu^-$ and $\mu^+\mu^-\gamma$ decays. The latter decay was evaluated with the probabilities corresponding to $E_{min} = 10$ MeV (points) and 200 MeV (histogram), respectively. The simulated mass resolution was about 42 MeV at the J/ψ peak.

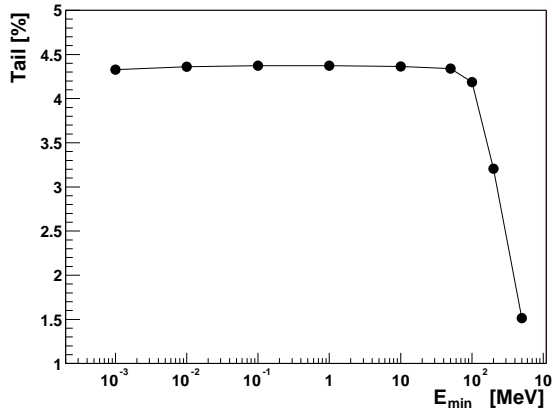


Figure 7: Fraction of events in the tail of dimuon mass spectra lower than 100 MeV as the J/ψ mass as a function of the cut parameter E_{min} . This fraction was evaluated for the mixture of $J/\psi \rightarrow \mu^+\mu^-$ and $\mu^+\mu^-\gamma$ decays simulated with probabilities corresponding to E_{min} . The mass resolution was about 42 MeV at the J/ψ peak.

On the one hand, E_{min} should not be extraordinarily small to stay away from the singularities in eqs.(6,7). On the other hand, the simulation with E_{min} much bigger than the mass resolution produces unreasonable mass spectra, as is clearly seen in fig. 6 for the spectrum simulated with $E_{min} = 200$ MeV and a mass resolution of 42 MeV. If the photon energy is small enough compared to the mass resolution σ , it does not matter whether l^+l^- or $l^+l^-\gamma$ was simulated, because the invariant mass is smeared with the resolution $\sigma \gg M - m$. The shape of the inclusive dilepton mass spectrum becomes stable against a decrease of E_{min} .

To make a proper choice we estimated the fraction of events in the “tail” of the dilepton mass spectra ($m < M(J/\psi) - 100$ MeV) as a function of the parameter E_{min} for decays $J/\psi \rightarrow \mu^+\mu^-$, $\mu^+\mu^-\gamma$ simulated with the mass resolution 42 MeV. This dependence, presented in fig. 7, shows a plateau where the results are stable with respect to the cut parameter E_{min} . We selected the value $E_{min} = 10$ MeV for further simulation.

4 Parameterisation of Smeared Mass Spectra

In this section the parameterisation of the smeared dilepton mass spectrum from the radiative decay (2) with $E_\gamma > E_{min}$ is given. The upper edge of the spectrum is the result of smearing of the sharp peak in the dilepton mass spectrum (14) at $m \approx M$ and it looks like a Gaussian (see fig. 5). For the full dilepton mass range we propose the following parameterisation:

$$\mathcal{P}(m) = G(m|m_R, \sigma_R), \quad m \geq m_S \quad (17)$$

and

$$\mathcal{P}(m) = c_S \cdot G(m|m_R, \sigma_S(m)), \quad m < m_S, \quad (18)$$

where $G(m|m_R, \sigma_R)$ is the Gaussian function

$$G(m|m_R, \sigma_R) = \frac{1}{\sqrt{2\pi} \sigma_R} \exp\left(-\frac{(m - m_R)^2}{2\sigma_R^2}\right)$$

with an average m_R and standard deviation σ_R , and $G(m|m_R, \sigma_S(m))$ that with standard deviation $\sigma_S(m)$, respectively, and c_S is a scaling factor. For a given mass resolution, the parameters m_R , σ_R and c_S are considered as constants, but $\sigma_S(m)$ as a polynomial:

$$\sigma_S(m) = \sum_i a_i^2 (m_R - m)^i \quad (19)$$

with constants a_i to be defined. Each term in the polynomial is positive which helps to reduce mutual correlations of parameters a_i during their search.

In the point $m = m_S$ we require continuity of the function $\mathcal{P}(m)$ and its first derivative $\mathcal{P}'(m)$. From the first condition we define the parameter c_S :

$$c_S = \frac{\sigma_S(m_S)}{\sigma_R} \exp\left(\frac{(m_S - m_R)^2}{2\sigma_S^2(m_S)} - \frac{(m_S - m_R)^2}{2\sigma_R^2}\right). \quad (20)$$

From the second condition follows the nonlinear equation

$$\left[\frac{1}{\sigma_S(m)} \frac{d\sigma_S(m)}{dm} + \frac{m - m_R}{\sigma_S^2(m)} - \frac{(m - m_R)^2}{\sigma_S^3(m)} \frac{d\sigma_S(m)}{dm} \right]_{m=m_s} = \frac{m_s - m_R}{\sigma_R^2} \quad (21)$$

to define m_S .

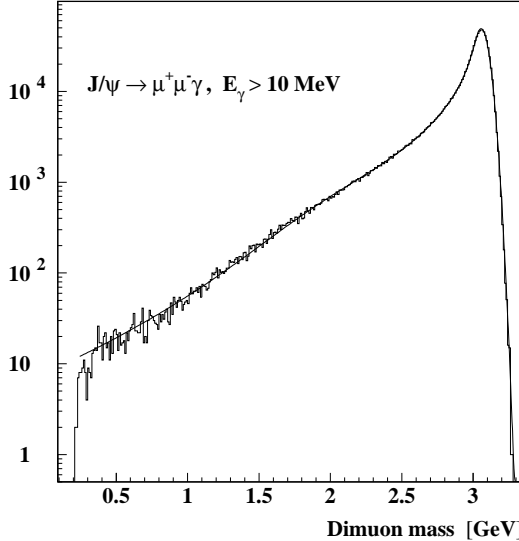


Figure 8: Monte Carlo results for the dimuon mass spectrum from the radiative decay $J/\psi \rightarrow \mu^+ \mu^- \gamma$ (histogram) and the parameterisation described in text (solid line). The simulation was made for a mass resolution of about 42 MeV at the J/ψ peak.

The remaining parameters m_R, σ_R, a_i were used as free parameters and determined from the condition of the best fit of $\mathcal{P}(m)$ to the dilepton mass distribution for 10^6 simulated radiative decays. For the decay $J/\psi \rightarrow \mu^+ \mu^- \gamma$ the parameters a_1, a_3, a_5, a_{10} were found to be statistically significant. The function $\mathcal{P}(m)$ with these parameters describe the simulated dimuon spectrum quite well, as seen in fig. 8.

We repeat the fitting of spectra simulated with different detector momentum resolutions and evaluated the dependences of the considered parameters as functions of the mass resolution $\sigma = \sigma(m)$ for $m = M$. Linear or quadratic polynomials in σ were sufficient to define these functions. The parameter σ is determined from the Gaussian fit of the $\mu^+ \mu^-$ mass spectra for independently simulated $J/\psi \rightarrow \mu^+ \mu^-$ decays.

The parameter σ_R depends linearly on the mass resolution as shown in fig. 9a). The nonlinearity of the parameter m_R is quite small as seen in fig. 9b). The point m_S , where the Gaussian distribution $G(m, m_R, \sigma_R)$ turns to the long tail, moves towards lower masses for a worse mass resolution (see fig. 10a). The coefficients of the polynomial (19) were rather well approximated by quadratic functions as presented in fig. 10b) for the parameter a_1 .

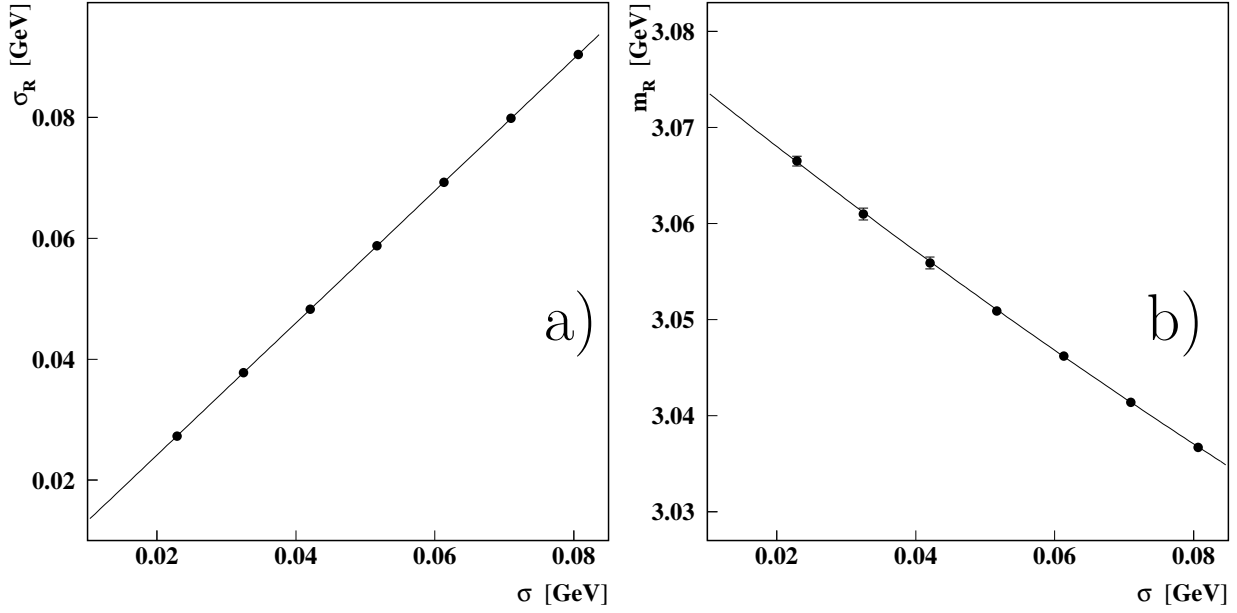


Figure 9: The parameters σ_R (a) and m_R (b) for the dimuon spectrum from the decay $J/\psi \rightarrow \mu^+ \mu^- \gamma$ as functions of the mass resolution σ .

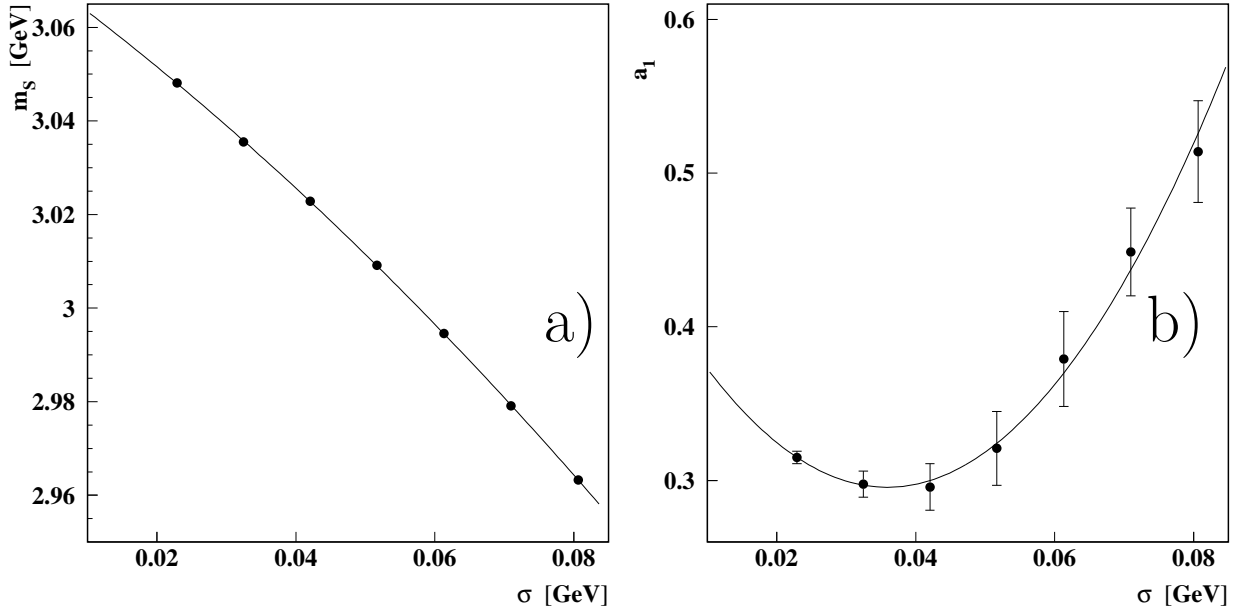


Figure 10: The parameters m_S (a) and a_1 (b) for the dimuon spectrum from the decay $J/\psi \rightarrow \mu^+ \mu^- \gamma$ as functions of the mass resolution σ .

Finally, we approximated as a quadratic polynomial in σ the factor

$$N_R(\sigma) = \frac{1}{\int \mathcal{P}(m|\sigma) dm} \quad (22)$$

to be used for normalisation of the function $\mathcal{P}(m|\sigma)$ for the given mass resolution.

As an example, we present the functional dependence for parameters determined for $J/\psi \rightarrow \mu^+\mu^-\gamma$ decays:

$$\begin{aligned}\sigma_R(\sigma) &= 0.22852 \cdot 10^{-2} + 1.0928 \cdot \sigma, \\ m_R(\sigma) &= 3.0795 - 0.58797 \cdot \sigma + 0.71851 \cdot \sigma^2, \\ m_S(\sigma) &= 3.0744 - 1.0624 \cdot \sigma - 3.9207 \cdot \sigma^2, \\ a_1(\sigma) &= 0.44397 - 8.2646 \cdot \sigma + 115.10 \cdot \sigma^2, \\ a_3(\sigma) &= 2.5218 - 14.572 \cdot \sigma + 479.51 \cdot \sigma^2, \\ a_5(\sigma) &= 3.3055 - 50.711 \cdot \sigma + 636.53 \cdot \sigma^2, \\ a_{10}(\sigma) &= 1.4641 - 9.2449 \cdot \sigma + 237.66 \cdot \sigma^2, \\ N_R(\sigma) &= 0.34397 + 7.2525 \cdot \sigma - 32.474 \cdot \sigma^2,\end{aligned}$$

where σ is varying from 0.023 to 0.081 GeV.

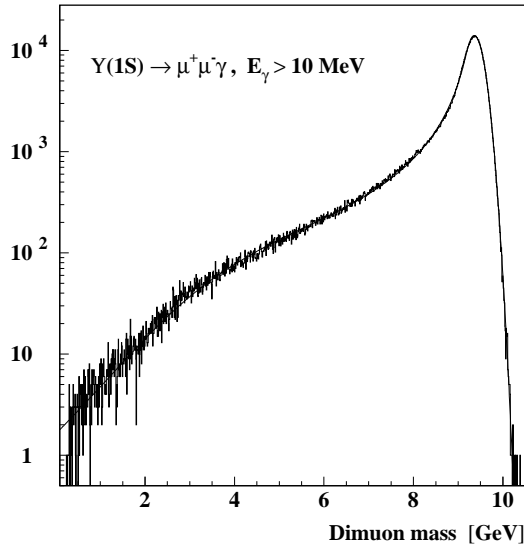


Figure 11: Monte Carlo results for the dimuon mass spectrum from the radiative decay $\Upsilon(1S) \rightarrow \mu^+\mu^-\gamma$ (histogram) and their parameterisation (solid line). The simulation was made for the mass resolution of about 176 MeV at the Υ peak.

The parameterisation describes also well the dimuon mass spectra simulated for the radiative decay $\Upsilon \rightarrow \mu^+\mu^-\gamma$ as seen in fig. 11. The shape of the tail looks more complicated than for the J/ψ . The shoulder around 4 GeV can be explained by acceptance effects for the simulated detector geometry. These effects appear in the mass range corresponding to very low values of $\mathcal{P}(m|\sigma)$. An additional parameter a_{20} was needed in polynomial (19) to overcome the complications of the mass spectrum.

Table 1: Sets of coefficients of the polynomial (19) found to be sufficient to parameterise inclusive dilepton mass spectra simulated for radiative decays of different particles.

Particle	Decay into $\mu^+\mu^-\gamma$	Decay into $e^+e^-\gamma$
J/ψ	a_1, a_3, a_5, a_{10}	$a_1, a_3, a_5, a_{10}, a_{20}$
$\psi(2S)$	a_1, a_3, a_5, a_{10}	$a_1, a_3, a_5, a_{10}, a_{20}$
$\Upsilon(1S)$	$a_1, a_3, a_5, a_{10}, a_{20}$	$a_1, a_3, a_5, a_{10}, a_{28}$

We simulated radiative decays of the $J/\psi, \psi(2S), \Upsilon(1S)$ into muon or electron pairs and evaluated the corresponding parameterisations for the dilepton spectra. In all cases, the parameters a_1, a_3, a_5, a_{10} were found to be significant as shown in table 1. For decays with smaller m_l/M an additional parameter was needed (a_{20} or a_{28}), to take into account specific details induced by the simulated experimental set-up. These parameters are needed at the lower edge of the mass spectra where the probability densities are low.

5 Treatment of Inclusive Measurements of Dilepton Mass Spectra

The dilepton mass spectra measured inclusively can be described as

$$S(m|M, \sigma) = (1 - W_{\text{hard}}) \cdot G(m|M, \sigma) + W_{\text{hard}} \cdot N_R(\sigma) \cdot \mathcal{P}(m|M, \sigma), \quad (23)$$

where $\mathcal{P}(m|M, \sigma)$ is the function (17,18) with corresponding parameterisation normalised by the factor $N_R(\sigma)$ and the weight W_{hard} defines the relative contribution of the radiative tail into the spectrum. The first term describes the configurations without photon and with low energies photons emissions smeared accordingly by detector resolutions. In a real experiment this term could be a more complicated function than a Gaussian. For electrons also an additional term could be appropriate to describe the bremsstrahlung process on the path through the detector material. As it was mentioned already, this process was not simulated for the present study. The weight W_{hard} can be defined as

$$W_{\text{hard}} = \frac{C_{\text{hard}}(E_{\text{min}}) \cdot A_{\text{hard}}(E_{\text{min}})}{(1 + C_{\text{soft}}(E_{\text{min}})) \cdot A_{\text{soft}}(E_{\text{min}}) + C_{\text{hard}}(E_{\text{min}}) \cdot A_{\text{hard}}(E_{\text{min}})}, \quad (24)$$

where $A_{\text{soft}}(E_{\text{min}})$ is an acceptance for l^+l^- and $l^+l^-\gamma$, ($E_\gamma \leq E_{\text{min}}$) final states and $A_{\text{hard}}(E_{\text{min}})$ that for $l^+l^-\gamma$, ($E_\gamma > E_{\text{min}}$). For close A_{soft} and A_{hard} the definition of W_{hard} by eq. (15) can be sufficient. The latter definition for $E_{\text{min}} = 10$ MeV we use for further calculations.

The corresponding mass spectra for the J/ψ decays are presented in fig. 12. The integral of the function (23) over the full interval of dilepton mass equals unity by definition. For the fitting of the histogram we used the product of the corresponding function (23)

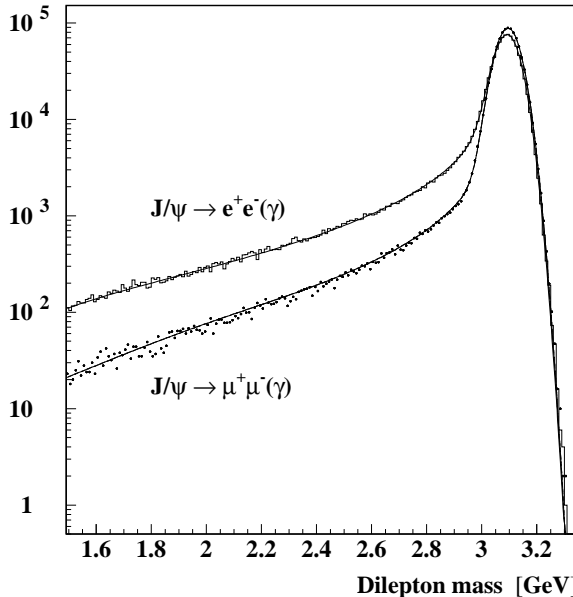


Figure 12: Monte Carlo results for inclusive dilepton mass spectra from decays of J/ψ into e^+e^- , $e^+e^-\gamma$ (histogram) and $\mu^+\mu^-$, $\mu^+\mu^-\gamma$ (points) and the fit curves using the parameterisations (23) (solid curves). The mass resolution was about 42 MeV at the J/ψ peak for both decays.

and the number of events treated as fit parameter. The function (23) itself depends on two parameters: the mass average M and resolution σ of the Gaussian part. Hence, there are three fit parameters in total.

The fitted curves describe well the results of the simulation as shown in fig. 12. The fitting procedures for decays of the $\psi(2S)$ shown in fig. 13a) and $\Upsilon(1S)$ in fig. 13b) were analogous to those described above. The fitting function also agreed with the simulation in a wide range of invariant masses.

To make a test on real data, we used the HERA-B data recorded with a dimuon trigger during the 2002–2003 HERA running period. Figure 14 shows the dimuon mass spectrum obtained from these data with a prominent signal above some background. The background was described by an exponential function.

In the HERA-B detector, a forward spectrometer with non-negligible amount of material on the path through the magnet [8], Molière scattering is essential [7] for the momentum resolution. Therefore in the fitting function (23) instead of one Gaussian we used a symmetric function composed of three Gaussians to take into account the details of the momentum (mass) resolution in the HERA-B detector. The fit of the dimuon mass spectrum by this symmetric function accompanied by an exponential function for the background resulted in $\chi^2 = 338$ for 108 degrees of freedom as presented in fig. 14a).

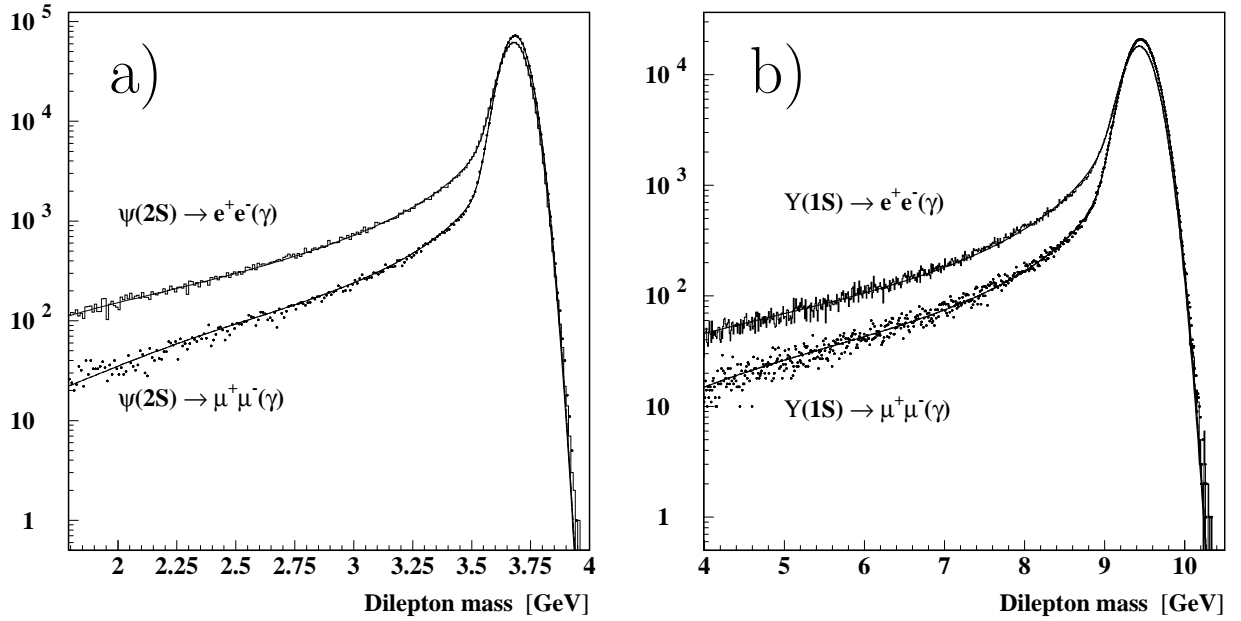


Figure 13: Monte Carlo results for inclusive dilepton mass spectra from onia decays into e^+e^- , $e^+e^-\gamma$ (histogram) and $\mu^+\mu^-$, $\mu^+\mu^-\gamma$ (points) and parameterisations (23)(solid curves). a) Decays of the $\psi(2S)$ were simulated with a mass resolution of 52 MeV at the signal peak. b) Decays of the $\Upsilon(1S)$ for a mass resolution of 176 MeV at the signal peak.

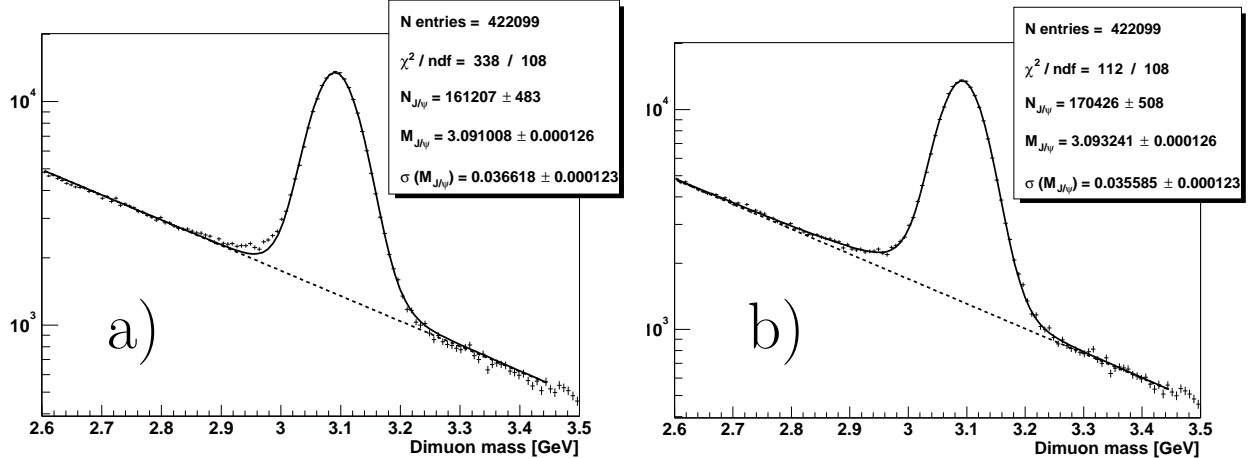


Figure 14: The invariant mass distribution of $\mu^+\mu^-$ around the J/ψ peak measured in the HERA-B experiment and fitted without the radiative tail taken into account (a) and with the parameterisation including the radiative tail (b). The values of χ^2 were 338 and 112, respectively, for 108 degrees of freedom. The background was described as exponential function (dashed curves). In inserts are shown: number of entries in the histogram, χ^2 , fitted number of J/ψ , fitted mass and mass resolution in GeV.

The inclusion of the radiative tail into the fitting function improved the result as seen in fig.14b), where $\chi^2 = 112$ for 108 degrees of freedom. One should remember that the radiative tail (second term in (23)) was defined through parameters of the first term, i.e. M and σ of the main peak, and the number of fitted parameters, and thus the degrees of freedom, were the same. Taking the radiative tail into account in the inclusive spectra of the dilepton mass could be significant for large statistics and rather high mass resolution.

6 Summary

Well known analytic results for the radiative decay of the vector boson $Z \rightarrow l^+l^-\gamma$ valid for arbitrary cuts in the photon energy and angles were used to estimate contributions of similar decays for charmonia and bottomonia vector states. The contributions were found to be rather large not only for decays into electrons but also into muons. The radiative effects appeared as tails in inclusive mass spectra of the lepton pairs. An analytic formula for the dilepton mass spectra in radiative decays is derived. The spectra convoluted with the detector mass resolution could be described by rather simple parameterisations. The parameterisations were studied by Monte Carlo for $J/\psi, \psi(2S), \Upsilon(1S)$ radiatively decaying into $\mu^+\mu^-\gamma$ or $e^+e^-\gamma$ using a simulation describing the real experiment. The parameterisation described the Monte Carlo results quite well and was found to be appropriate also for fitting real data.

Acknowledgments: I had great benefit from the expertise and advices of F. Jegerlehner whose detailed analytic results for radiative decays of Z bosons were the starting point for this study. Cordial thanks to T. Lohse who stressed the importance of radiative decays for charmonia measurements and developed the Monte Carlo generator used for the investigation. Fruitful discussions with G. Bohm and H. Kolanoski helped me a lot to finalize the results. I am also grateful to them for the careful reading of the manuscript. I would like to thank DESY Zeuthen for the kind hospitality extended to me during my visit.

References

- [1] J. Fleischer and F. Jegerlehner, *Radiative $Z-$ and $W^\pm-$ Decays: Precise Prediction from the Standard Model*, Z. Phys. C26 (1985) 629.
- [2] W. Buchmüller and S. Cooper, Υ Spectroscopy, in Advanced Series on Directions in High Energy Physics – Vol.1(p.412), *High Energy Electron-Positron Physics*, Ed. A. Ali and P. Söding, World Scientific (1988).
- [3] T.A. Armstrong et al., *Observation of the radiative decay $J/\psi \rightarrow e^+e^-\gamma$* , Phys. Rev., D54 (1996) 7067;

- [4] T. Lohse et al. (HERA-B Collaboration), DESY-PRC 94/02 (1994).
- [5] T. Lohse, *FORTRAN program for simulation of radiative decays of J/ψ* , private communication.
- [6] J. Ivarsson, P. Kreuzer and T. Lohse, *PYTHIA and FRITIOF: Event Generators for HERA-B*, HERA-B note 99-067 (1999).
- [7] A. Spiridonov, *Momentum and Angular Resolutions in the HERA-B Detector*, HERA-B note 02-069 (2002).
- [8] A. Spiridonov, *Uncertainties in Track Momentum due to Multiple Scattering in a Forward Spectrometer*, Preprint DESY 02-151(2002).